Mathematical Biosciences and Engineering

https://www.aimspress.com/journal/mbe

MBE, 23(1): 148–171.
DOI: 10.3934/mbe.2026007
Received: 12 August 2025
Revised: 07 October 2025
Accepted: 31 October 2025
Published: 02 December 2025

Research article

Self-organized social distancing during epidemics when the force of infection depends on susceptible and infectious behavior

Simon K. Schnyder [1,*], John J. Molina [2], Joel C. Miller [3,4], Ryoichi Yamamoto [2], Tetsuya J. Kobayashi [1,5,6] and Matthew S. Turner [7,8,*]

[1] Institute of Industrial Science, The University of Tokyo, Tokyo 153-8505, Japan

[2] Department of Chemical Engineering, Kyoto University, Kyoto 615-8510, Japan

[3] Department of Mathematics and Physical Sciences, La Trobe University, Bundoora, VIC 3086, Australia

[4] Australian Centre for Artificial Intelligence in Medical Innovation, La Trobe University, Bundoora, VIC 3086, Australia

[5] Universal Biology Institute, The University of Tokyo, Tokyo 113-0033, Japan

[6] Department of Mathematical Informatics, Graduate School of Information Science and Technology, The University of Tokyo, Tokyo 113-8656, Japan

[7] Department of Physics, University of Warwick, Coventry CV4 7AL, UK

[8] Institute for Global Pandemic Planning, University of Warwick, Coventry CV4 7AL, UK

* **Correspondence:** Email: skschnyder@gmail.com (SKS); m.s.turner@warwick.ac.uk (MST).

Abstract: During epidemics, individuals may adjust their social behavior in response to the threat. This may affect the course of the epidemic, and, in turn, again modify people's behavior. Game theoretically, the system may end up in a Nash equilibrium, where no member of the population can benefit by unilaterally changing their behavior. Compartmentalized epidemic models can incorporate such endogenous decision making, where individuals try to optimize a utility function via their behavior. Typically, such models can only be solved numerically. Here, we extend a recently discovered analytic solution for time-dependent social distancing and the corresponding epidemic dynamics: now, the probability of an infection taking place can depend on both the susceptible and infectious individual behaviors. We show that the more effectively the susceptible individual can reduce the probability of infection, the more self-organized social distancing is expected to occur. The previously identified heuristic that the strength of rational social distancing is proportional to both the perceived infection cost and prevalence is found to also hold in the generalized model.

Keywords: mathematical epidemiology; mean-field games; control theory

1. Introduction

Many infectious diseases spread within a given population via contacts between infectious and susceptible individuals. Given how harmful diseases can be, individuals might want to modify their behavior to reduce the chances of disease transmission. While early compartmental models of epidemics [1] did not consider such behavioral dynamics, this soon became the focus of research, e.g. [2–6]; for reviews, see [7–12]. Understanding the interplay of epidemic and behavioral dynamics is a central question in epidemiology, and it has been shown that models that incorporate behavioral components perform better than purely data-driven approaches when fitting to data [13]. Behavioral models have furthered the understanding of epidemics such as COVID-19 [13] or HIV [14].

Philosophies for modeling behavior widely vary [7–9, 12, 15], ranging from agent behavior being determined by the state of the epidemic ad-hoc, to agents imitating other agents, to governments or other decision makers imposing limitations on behavior, to economics-inspired frameworks where behavior is motivated by the aim to optimize an objective function [16].

Driven by the goal of accurately reproducing epidemic dynamics, epidemic models can become arbitrarily complex, such as by including sophisticated compartmental structures representing age [17–21] or multiple infection states [22], agent-based modeling [23–26], spatial and temporal networks [27–29], spatial structure, seasonality [30], heterogeneity [31–36], vital dynamics, loss of immunity [21, 37, 38], stochasticity [39–42], uncertainty [43, 44], or intervention by governments [8, 16, 45–50]. Such complex models tend to only be solvable numerically and it can be challenging to explore all of their features. On the other hand, the benefit of more idealized models is that there might be an avenue for analytic study, with all the deep insights that bestows. However, analytic solutions for compartmental disease models have been mostly restricted to constant reproduction ratios [1, 51–55] and therefore could not express dynamic behavior.

Recently, an analytic solution was found for an idealized compartmental behavioral epidemiology model [56]. In this model, social distancing behavior of individuals arises out of a game-theoretic treatment of their interests in a fully time-dependent manner. The present work is a generalization of this prior research. We assume that individuals aim at maximizing an individual objective function given the course of the epidemic, itself determined by the general population's behavior. If the other individuals making up the population have the same goals in mind, then the population's behavior ends up in a Nash equilibrium [3]. This outcome tends not to reach the global maximum of the objective function, but has the benefit that it is stable against defection by free-riders. Reaching the global maximum would typically require coordination between individuals [45, 57–59] or intervention by a decision maker such as a government [8, 16, 58, 60–62], e.g. via tax and subsidy incentives [63].

We formulate the decision making problem for social distancing as a mean-field game [64, 65] from the viewpoint of a representative individual making choices about their own social behavior. The disease dynamics are given by a simple compartmental susceptible-infectious-recovered (SIR) model. The average social activity of the population dynamically determines the infection rate within the population and is considered to be an exogenous quantity, outside of the control of the individual who can only control how they personally react to the course of the epidemic. The individual can invest in social distancing at a cost, thereby reducing their probability of getting infected.

Ultimately, we are interested in the special case in which all population members are identical and all individually react to the course of the epidemic in the same way. This leads to a Nash equilibrium in

which the population behavior ends up equal in value to the representative individual's behavior. However, for a game-theoretic analysis it is necessary to independently consider individual and population behaviors at the outset.

We assume that the transmission rate can depend even non-linearly on the time-dependent social behaviors of both the susceptible and the infectious. Earlier work with a similar transmission rate model is e.g. [4, 60, 66], albeit focused on numerical results. In principle, the model allows for the behaviors of susceptible and infectious to be different. Later, we assume that all compartments exhibit the same behavior in order to be able to calculate an exact and time-dependent analytic solution for the behavior and the disease dynamics for the Nash equilibrium. In [56], only the susceptible behavior affected the transmission rate.

Our results reduce to the previously known solution of the SIR model [1, 51–54] if the individual decides not to adjust their behavior, either because the infection cost is vanishingly small or because their behavior has a vanishingly small effect on their probability of getting infected.

In order to achieve an analytic solution, we made a range of modeling choices: while our approach is quite similar to some previous studies [3, 57, 62, 67–69], there are a few main differences that need discussing. The cost of infection is assumed to be constant – a common assumption [3, 57, 67–69] – and ignores aspects such as limited hospital capacity [62]. The cost of social distancing is assumed to be quadratic in the reduction of social activity away from the default behavior. In principle, this means that the disease can be stopped from spreading at a finite cost per time. This unrealistic feature of the model could be remedied with a cost that diverges for perfect social distancing [3]. However, given that self-organized behavior cannot achieve disease eradication [8, 16, 70], the lack of a divergence in the cost term can be ignored in this work. As a result, we only study the scenario that leads to herd immunity. Furthermore, we assume that the cost of social distancing is paid by the individual regardless of which compartment they are in (somewhat similarly to [67]). This corresponds to an individual who does not know (well) which compartment they are in. This would hold for infections that can be (at first) largely asymptomatic, but end up being costly (in the long run), such as COVID-19, Epstein-Barr, HIV, Herpes, or HPV. While the individual is not well aware of their infection status, we assume that the state of the epidemic be perfectly known at any moment. For instance, this can be realized in a situation where techniques such as sewage testing [71] provide good information about the course of the epidemic, while individual fates are less well known. In addition, people might respond to hospitalization rates. If most cases are asymptomatic, then the vast majority would be unaware of their own status but respond to information about prevalence through the small symptomatic proportion. Qualitatively, we find that our results are largely comparable to the typically studied scenario of paying for and engaging in social distancing only when susceptible [3, 69]. The most obvious difference is that we predict that social distancing is the most extreme at the peak of the epidemic, while approaches where only the susceptible social distance predict that the peak of social distancing happens after the peak of the epidemic. While we had to make many idealizations in order to obtain a solvable model, the results are qualitatively in agreement with more complex models. Therefore, our hope is that insights gained from our analytic solution may help both in the general understanding of self-organized behavior during epidemics and help governments in their decision making.

2. Model

2.1. Epidemic dynamics in the general population

The epidemic dynamics are described by a standard SIR compartmental model [1], with the population consisting of susceptible $s(t)$, infectious $i(t)$, and recovered $r(t)$ compartments. The dynamics of the compartments are given as follows:

$$\begin{aligned}\frac{d}{dt}s(t) &= -R_b(t)\, s(t)\, i(t),\\ \frac{d}{dt}i(t) &= R_b(t)\, s(t)\, i(t) - i(t),\\ \frac{d}{dt}r(t) &= i(t),\end{aligned} \tag{2.1}$$

with the *behavioral reproduction number* $R_b(t)$ that depends on the behavior of the population as specified further below. Time dependences (e.g. of $s(t)$, $i(t)$, $r(t)$ and $R_b(t)$) are typically omitted for brevity in what follows. Because we ignore births and natural deaths, and include deaths from the disease in r, the compartments can be normalised, $1 = s + i + r$. We rescaled the equations so that time t is measured in units of the duration of a typical infection. The initial conditions are given as $s(0) = s_0$, $i(0) = i_0$, and $r(0) = r_0$ with $s_0, i_0, r_0 \geq 0$ and $s_0 + i_0 + r_0 = 1$.

We define the behavioral reproduction number as follows:

$$R_b = R_0\, k_s^x\, k_i^y, \tag{2.2}$$

with the basic reproduction number R_0, the susceptible population behavior k_s, the infectious population behavior k_i and two exponents, x for susceptible and y for infectious behavior. The exponents x and y control how strongly the behavior affects the transmission rate, and will be referred to as the *effectiveness* of the respective social distancing. The activity terms k_s^x and k_i^y enter as a product analogous to how the rate of new infections in Equation (2.1) is a product of s and i. This corresponds to assuming that the effects of the respective activities on R_b are independent from each other. Since the behaviors do not necessarily have to enter the dynamics symmetrically or even linearly, we allow x and y to have different, non-negative values. In what follows, we assume that all individuals of the population exhibit the same behavior regardless of the compartment they currently find themselves in, $k_s = k_i = k_r = k$. This corresponds to the assumption that the disease is asymptomatic. We found that we were not able to calculate an analytic solution without this assumption. The population's average social activity in the absence of an epidemic is assumed to correspond to $k = 1$. Additionally, one must also demand that $k \geq 0$ on plausibility grounds. Later, we will show that the range of behavior is naturally more constrained than that.

Now, we can write the population dynamics as

$$\begin{aligned}\frac{d}{dt}s &= -R_0 k^{x+y}\, s\, i,\\ \frac{d}{dt}i &= R_0 k^{x+y}\, s\, i - i,\\ \frac{d}{dt}r &= i.\end{aligned} \tag{2.3}$$

These equations can only be evaluated once we have found an expression for the behavior k. This will be the focus of the following sections.

2.2. *Individual decision making yields a Nash equilibrium*

With the goal of studying self-organized behavior, we single out a representative individual and their behavior. By reacting to the population behavior k and the corresponding epidemic dynamics (in particular i), the individual can influence their own fate with their social distancing behavior $\kappa(t) \geq 0$. In this work, we neglect the extremely small effect of the individual on the epidemic. The probabilities of the individual being in each of the compartments obey

$$\begin{aligned} \frac{d}{dt}\psi_s &= -R_0\kappa^x k^y \psi_s i, \\ \frac{d}{dt}\psi_i &= R_0\kappa^x k^y \psi_s i - \psi_i. \end{aligned} \tag{2.4}$$

These equations slightly differ from Equations (2.3), to reflect that the individual is solely infected by the population. We can ignore the trivial dynamics for the probability ψ_r of recovery in what follows.

The individual can lower their probability of becoming infected by reducing their activity $\kappa(t)$. However, in general, a reduction of activity will lead to a social or economic cost for that individual. This tradeoff can be mathematically expressed with an objective function or utility U which the individual is trying to maximize. We use an idealized form for U as follows:

$$U(\kappa, k) = \int_0^{t_f} u(t)dt + U_f, \tag{2.5}$$

$$u = -\alpha\,\psi_i - (\kappa^z - 1)^2, \tag{2.6}$$

with an exponent $z > 0$. The utility represents the expected total costs for the individual integrated over the whole duration of the epidemic. In particular, the notation is meant to emphasize that the utility depends on the population and individual behaviors. When infected, the individual pays an expected infection cost $\alpha \geq 0$. The expected cost of death can be absorbed into α as well. Deviating from one's personal default behavior $\kappa = 1$ is associated with social and economic costs. Later, we focus on the special case $z = 1$, so that this cost grows quadratically when deviating from the default behavior. This is a common choice in control theory, but not the only plausible one [3]; for instance, others prefer a cost that diverges as $\kappa \to 0$, but this feature would not play an important role in this work. We have introduced the exponent z into the utility to facilitate analytic solution of the problem. As far as we are aware, the solution developed in the following requires that $z = x + y$. Without loss of generality, we chose to scale the utility such that the cost of complete social distancing for one time unit is given by 1 (i.e. one unit of utility). In this sense, α measures how costly an infection is compared to complete social distancing for one disease generation. Note that the definition of the utility slightly differs from that given in [56]: for $x = z = 1$ and $y = 0$, a given value of α here corresponds to an infection cost of value αR_0^2 there. At a final time t_f, we assume that the remaining susceptible fraction of the population becomes instantaneously vaccinated and thus immune to the disease. This is a common choice [3, 18, 57, 69] that helps with obtaining a well-defined boundary value problem to solve. If one is infected at $t = t_f$, one still has to recover in the usual way, which implies a cost [56] as follows:

$$U_f = -\alpha\,\psi_{i,f} \tag{2.7}$$

We only study the case in which t_f is large enough so that $\psi_{i,f} \approx 0$.

A rational individual will seek to maximize this objective function by choosing their own behavior κ for a given population behavior k. If the population consists of like-minded individuals with the same goals, then a situation can arise in which the population average behavior becomes fully aligned with the behavior of the individual, $k(t) = \kappa(t)$. In that situation, the individual cannot improve their outcome by unilaterally changing their behavior, such that

$$U(\tilde{\kappa}(t), \kappa(t)) \leq U(\kappa(t), \kappa(t)) \quad \text{for any } \tilde{\kappa}(t). \tag{2.8}$$

This represents a Nash equilibrium, which can be identified as follows. One first optimizes the utility over the individual behavior κ for an arbitrary, exogenous k (which also uniquely determines the population disease dynamics). After that, one identifies the special case in which $k = \kappa$. As a result, $\psi_s = s$, $\psi_i = i$, too. Formally,

$$k = \left[\arg\max_{\kappa} U(\kappa, k) \quad \text{subject to Equations (2.3) and (2.4)} \right]_{\kappa=k}. \tag{2.9}$$

2.3. Restatement of the optimization as a boundary value problem

The problem stated in Equation (2.9) represents a standard constrained optimization problem [72, 73] of a mean-field game. Typically, one first restates this as an unconstrained problem, and then transforms it into a boundary value problem that can be solved with standard techniques. This is an exact approach. In optimal control theory, the procedure is known as Pontryagin's maximum principle [72–74], whereas physicists would know it as Hamiltonian/Lagrangian formalism. For a discussion of the derivation of the approach, see [72, 73] or Supplementary Information in [62]. The approach requires the definition of a helper function, a Hamiltonian, that is then used to derive a set of differential equations. The Hamiltonian is defined as follows:

$$\begin{aligned} H &= u + v_s \frac{d\psi_s}{dt} + v_i \frac{d\psi_i}{dt} = u + v_s(-R_0 \kappa^x k^y \psi_s i) + v_i(R_0 \kappa^x k^y \psi_s i - \psi_i) \\ &= -\alpha\psi_i - (\kappa^z - 1)^2 - (v_s - v_i) R_0 \kappa^x k^y \psi_s i - v_i \psi_i. \end{aligned} \tag{2.10}$$

The Lagrange multipliers or costates $v_s(t)$ and $v_i(t)$ express the expected present value of the utility of being in each compartment at each point in time [72]. Additionally, they make sure that the optimized dynamics still satisfy the epidemic equations, see Equations (2.4). Their dynamics are given by the following:

$$\frac{d}{dt} v_s = -\frac{\partial H}{\partial \psi_s} = (v_s - v_i) R_0 \kappa^x k^y i, \tag{2.11}$$

$$\frac{d}{dt} v_i = -\frac{\partial H}{\partial \psi_i} = \alpha + v_i, \tag{2.12}$$

with the boundary conditions

$$v_s(t_f) = \frac{\partial U_f}{\partial \psi_{s,f}} = 0, \qquad v_i(t_f) = \frac{\partial U_f}{\partial \psi_{i,f}} = -\alpha. \tag{2.13}$$

In reaction to the state of the epidemic as described in particular by k and i, the individual chooses the behavior κ that optimizes their utility. Said behavior is given by the following:

$$0 = \frac{\partial H}{\partial \kappa} = -2z\kappa^{z-1}(\kappa^z - 1) - (v_s - v_i)R_0 x\kappa^{x-1}k^y\psi_s i \tag{2.14}$$

Note that this behavior also depends on $(v_s - v_i)$, which is the perceived difference in utility of staying susceptible as compared to becoming infected. In order to find the Nash equilibrium, we now assume that the population behavior arises because the population consists of individuals with identical preferences all rationally choosing the same behavior; therefore, $k = \kappa$, and hence $s = \psi_s$ and $i = \psi_i$. Then, Equation (2.14) reduces to the following:

$$0 = -2zk^{z-1}(k^z - 1) - (v_s - v_i)R_0 xk^{x+y-1}si. \tag{2.15}$$

In order to make full analytic progress, it is convenient to set $z = x + y$. Other choices for the exponent are possible. For some choices, partial analytic results are accessible, see Appendix. Then, since $k > 0$, we see that

$$k^{x+y} = 1 - \frac{R_0 x}{2(x+y)}(v_s - v_i)si; \tag{2.16}$$

therefore,

$$R_b = R_0 k^{x+y} = R_0 - \frac{R_0^2 x}{2(x+y)}(v_s - v_i)si. \tag{2.17}$$

Choosing $z = x + y$ has the further advantage that the value function (i.e. the objective function evaluated at the Nash equilibrium) then has a quadratic dependence on the behavioral modification away from the pre-epidemic baseline as follows:

$$V(t) = \int_t^{t_f} -\alpha i - \left(\frac{R_b(t) - R_0}{R_0}\right)^2 dt - \alpha i_f. \tag{2.18}$$

This guarantees convexity in R_b and represents the simplest plausible social distancing cost: for any social distancing cost that is analytic in R_b near $R_b = R_0$, one would expect the lowest order term to enter at quadratic order in $R_b - R_0$, unless fine-tuned so that this term precisely vanishes.

3. Analytic solution

The behavior and corresponding epidemic dynamics in the Nash equilibrium are given by the solution of Equations (2.3), (2.11) to (2.13), and (2.17). From here, we calculate the analytic solution for this set of equations. Because the total fraction of recovered cases $r(t)$ monotonically increases with time t,

$$r = \int_0^t i(t')dt' + r_0, \tag{3.1}$$

we can express the differential equations in terms of r instead of t. This or similar reparametrizations of time are a common technique in the analysis of epidemic compartmental models (e.g. see [51–53, 75]). With $dr/dt = i$, we rewrite the set of equations to be solved as follows:

$$\frac{d}{dr}s = -R_b\, s, \tag{3.2}$$

$$\frac{d}{dr}i = R_b\, s - 1, \tag{3.3}$$

$$\frac{d}{dr}v_s = (v_s - v_i)R_b, \tag{3.4}$$

$$\frac{d}{dr}v_i = \frac{\alpha + v_i}{i}, \tag{3.5}$$

$$R_b = R_0 - \frac{R_0^2 x}{2(x+y)}(v_s - v_i)si. \tag{3.6}$$

By defining

$$K(r) = \int_{r_0}^{r} R_b(r')dr', \tag{3.7}$$

the susceptible fraction is directly given by

$$s = s_0 e^{-K(r)}. \tag{3.8}$$

Using the normalization $s + i + r = 1$, we obtain the following:

$$i = 1 - r - s_0 e^{-K(r)}. \tag{3.9}$$

We exploit that $i = dr/dt$ and integrate this equation to derive the mapping between r and t as follows:

$$F(r) \equiv \int_{r_0}^{r} \frac{dr'}{1 - r' - s_0 e^{-K(r')}} = t \quad \text{hence} \quad r = F^{-1}(t). \tag{3.10}$$

Next, we remind ourselves that we only focus on the case where t_f is large enough that $i(t_f) \to 0$. This can be used to simplify Equation (3.9) in order to find an expression for the final fraction of recovered (i.e. the cumulative total of infections),

$$r_f + s_0 e^{-K(r_f)} = 1. \tag{3.11}$$

Equations (3.1) and (3.7) to (3.11) hold for any time-dependent behavior $R_b(t)$ and thus are true for any reasonable choice of objective function. However, it would seem that an explicit analytic solution is only possible for special cases, such as ours, Equation (2.6).

The Lagrange multiplier v_i has the simple solution $v_i(r) = -\alpha$, as can be directly seen from inspecting Equation (3.5). The other Lagrange multiplier v_s follows from rewriting Equation (3.4),

$$\frac{d}{dr}v_s = (v_s + \alpha)\frac{d}{dr}K. \tag{3.12}$$

We integrate this and find the following:

$$v_s + \alpha = \mu e^K = \mu \frac{s_0}{s}, \tag{3.13}$$

with a constant μ. Using the boundary condition $v_s(t_f) = v_s(r_f) = 0$ with $s_f = s(r_f)$, we obtain the following:

$$v_s = \alpha \frac{s_f}{s} - \alpha. \tag{3.14}$$

The Nash equilibrium behavior is obtained by inserting the Lagrange multipliers into Equation (2.17) as follows:

$$R_b = R_0 - \frac{x}{2(x+y)} R_0^2 \alpha s_f i. \tag{3.15}$$

This is a strikingly simple result: in our model, it is rational to target a reduction in the reproduction number $R_b - R_0$ that is proportional to, in particular, the current disease prevalence i.

Proceeding further, we insert Equation (3.15) and $i = 1 - r - s$ into Equation (3.2) and obtain the following:

$$\begin{aligned} \frac{ds}{dr} &= -s[R_0 - \frac{xR_0^2 \alpha s_f}{2(x+y)}(1-r-s)] \\ &= -s[a + br + bs], \end{aligned} \tag{3.16}$$

with $a = R_0 - b$ and

$$b = \frac{x}{2(x+y)} R_0^2 \alpha s_f. \tag{3.17}$$

Equation (3.16) can be analytically solved by the following:

$$s(r) = \frac{\exp\left[-\frac{1}{2}(r-r_0)(2a + b(r+r_0))\right]}{\frac{1}{s_0} - \sqrt{\frac{\pi b}{2}} e^{\frac{(a+br_0)^2}{2b}} \left(\mathrm{Erf}\left[\frac{a+br_0}{\sqrt{2b}}\right] - \mathrm{Erf}\left[\frac{a+br}{\sqrt{2b}}\right]\right)}, \tag{3.18}$$

with $s(r \to r_0) \to s_0$. This expression still depends on r_f; however this can be easily self-consistently determined via $r_f = 1 - s(r_f)$. Formally, this result appears unchanged from the solution presented in [56], but depends here on the effectivenesses x and y via the adjusted definition of b.

4. Results

For the presentation of our results, we chose initial conditions where social distancing is still negligibly small, $r(0) = i(0)/(R_0 - 1) = 10^{-6}$ with $s(0) = 1 - i(0) - r(0)$. There is considerable freedom in choosing the effectiveness x of susceptible individual social distancing and the effectiveness y of infectious population social distancing. For simplicity, we restrict ourselves to the case in which $x + y = 1$ from now on. In that case, $R_b = R_0 k$, and we can straightforwardly discuss the behavior in terms of k.

The central result of this paper is that we have been able to extend the full analytic solution derived in [56] to more realistic infection dynamics, see Equation (3.18). See Figure 1(a,c,e) for a direct plot of this solution for a range of x. While this solution is given in terms of the recovered fraction r, it can be straightforwardly presented as a function of time via Equation (3.10), see Figure 1(b,d,f). We note that the higher the effectiveness x of susceptible social distancing, the more social distancing is observed. Our previous work [56] corresponds to dark lines for $x = 1$. An effectiveness of $x = 1$ yields the strongest incentive to social distance, as it assumes that the susceptible fraction is in complete control of the behavioral reproduction number, whereas the behavior of the infectious is irrelevant. An effectiveness of $x = 0$ results in no behavioral modification, as it assumes that the infectious

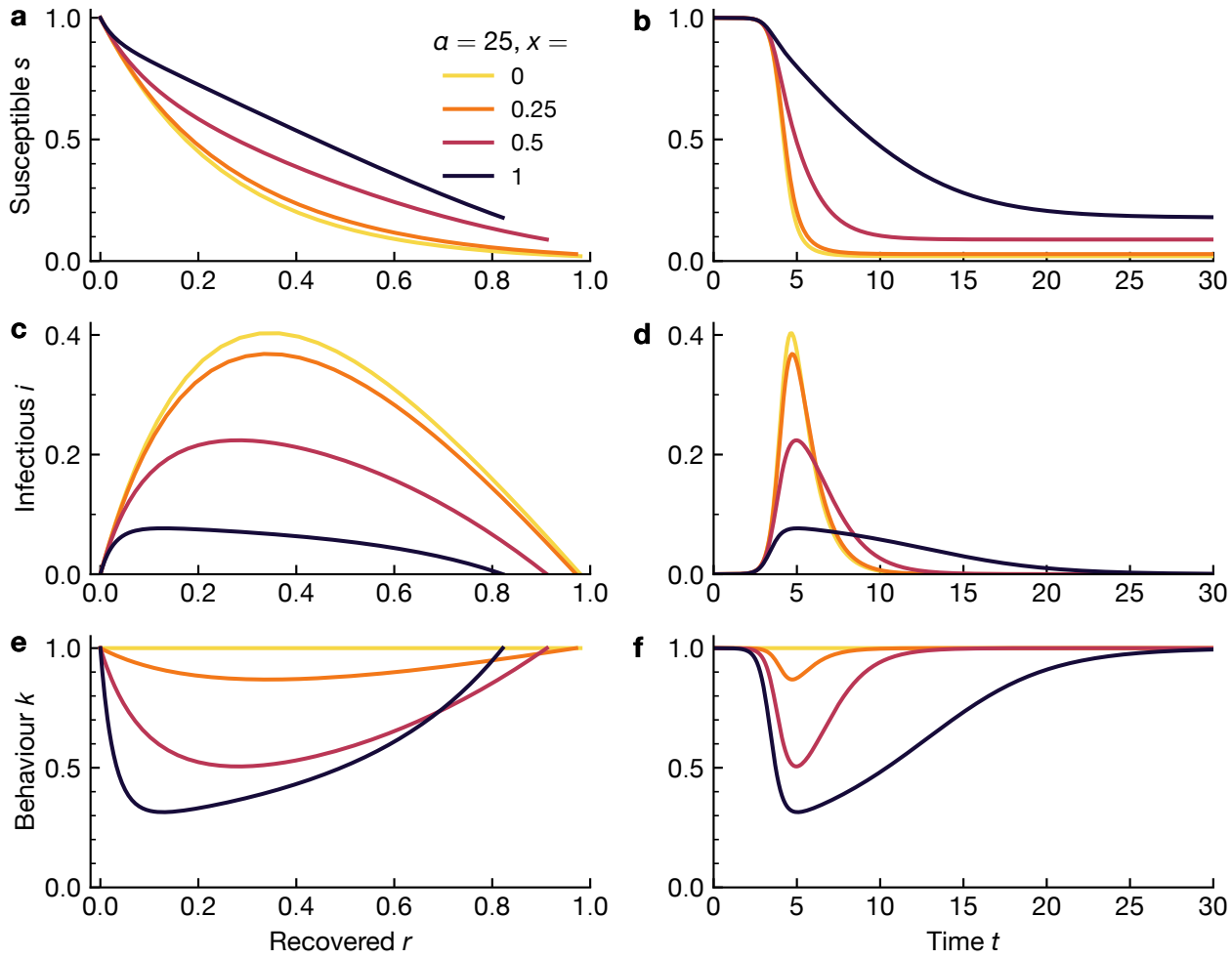

Figure 1. Plots of the solution. Analytic solution of the Nash equilibrium social distancing problem, Equation (3.18) for an infection cost $\alpha = 25$ and a range of effectiveness x of the susceptible individual social distancing with the social distancing effectiveness of the infectious population given by $y = 1 - x$. The x values are color coded consistently across all figures. As a function of the recovered r, we show the susceptible fraction (a), the infectious fraction (c), and the population behavior (e). As a function of time t, we show the susceptible fraction (b), the infectious fraction (d), and the population behavior (f). In all figures, the initial conditions are set to $r_0 = 10^{-6}$, $i_0 = 3 \cdot 10^{-6}$, and the basic reproduction number $R_0 = 4$.

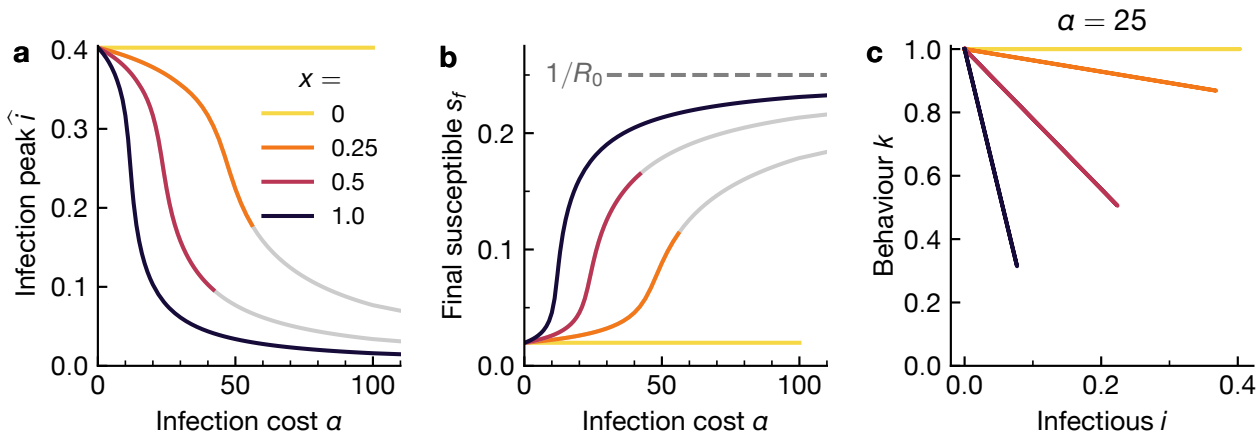

Figure 2. The dynamics undergo a transition from weak to strong social distancing. (a) Infection peaks $\hat{i}$ as a function of infection cost α for a range of effectiveness x. The light grey lines in this figure indicate where the solution does not represent a Nash equilibrium, as will be discussed further below in Section 4.1. (b) Final fraction of susceptibles s_f as a function of α for a range of x. For large α, $s_f \to 1/R_0$, see the grey dashed line. (c) The linear relationship between rational behavior k and infectious fraction i is demonstrated for a range of x for constant $\alpha = 25$.

fraction is in complete control of the behavioral reproduction number: This results in the situation where a susceptible individual cannot affect their probability of becoming infected, while an infected individual is always powerless to affect their fate. As a result, the self-interested individual will not take any action. However, in general, one would expect an effectiveness between these two limits, $0 < x < 1$. In particular, one would assume that the situation in which both susceptible and infectious behavior equally contribute to the infection probability is most representative of real diseases.

The higher α or x are, the stronger the effort towards social distancing. As a result, the epidemic progresses more slowly, the infection peak becomes reduced, Figure 2a, and the fraction that remain uninfected at the end of the epidemic s_f grows, Figure 2b. The linear relationship between the current rational social distancing behavior and the current prevalence, Equation (3.15), is shown in Figure 2c.

In Figure 2, we see how quantities such as the infection peak and s_f undergo a transition as a function of α and x. This can be analyzed in more detail, and in particular, we will identify two limiting cases:

(1) The *non-behavioral limit*. Here, either infections are perceived to not carry a cost, $\alpha = 0$, or one's behavior has no effect on one's infection probability, $x = 0$. Therefore, in this limit there is no modification of behavior, $k = R_0$, see yellow lines in Figure 1.

(2) The *strong social distancing limit*. Here, the infection costs and the effectiveness of social distancing are very high.

Two central quantities allow us to effectively investigate these regimes: the excess cases ε and the peak of the epidemic $\hat{i} = \max(i)$. We can obtain the crossover between these two regimes by matching their asymptotes. This will yield two crossover costs.

The excess cases ε are given by the number of infections at $t = t_f$ in excess of the herd immunity

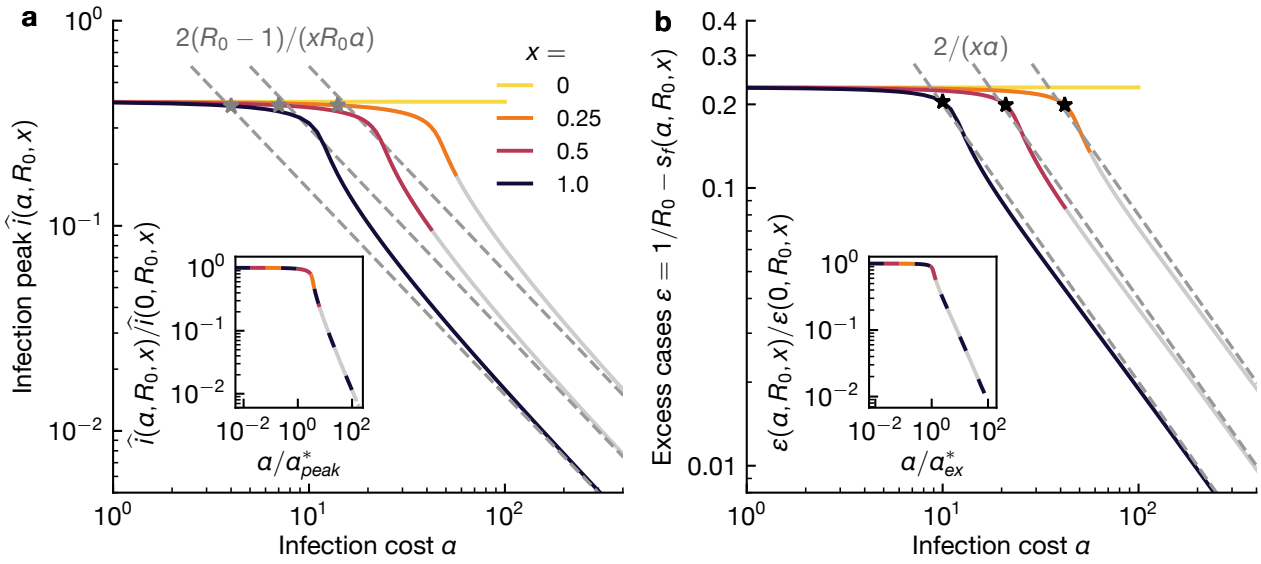

Figure 3. Scaling using analytic asymptotes for the non-behavioral and strong social distancing limits. (a) The infection peak $\hat{i}$ as a function of the infection cost α for a range of effectiveness x at $R_0 = 4$. The light grey solid lines in the figure indicate where the solution does not represent a Nash equilibrium, as discussed in Section 4.1. The high infection cost asymptotes, see Equation (4.7), are shown as dashed lines and the crossover costs $\alpha^\star_{peak}$, see Equation (4.10), as grey stars. Inset: The data collapses onto a single curve by rescaling the cost α with the crossover cost $\alpha^\star_{peak}$, Equation (4.10), while rescaling the peak height with its non-behavioral limit, see Equation (4.5). Here, the data is shown as dashed lines, as they would otherwise completely overlap. (b) Excess cases $\varepsilon(\alpha, R_0, x)$ as a function of infection cost α for a range of x. The high infection cost asymptotes, see Equation (4.6), are shown as dashed lines and the crossover costs $\alpha^\star_{ex}$, see Equation (4.9), as black stars. Inset: The data collapses onto a single curve by rescaling the cost α with the crossover cost $\alpha^\star_{ex}$, see Equation (4.9), while rescaling $\varepsilon(\alpha, R_0)$ with its non-behavioral limit, see Equation (4.4). Here, the data is shown as dashed lines, as they would otherwise completely overlap.

threshold $1 - 1/R_0$. In terms of the susceptible fraction, this can be written as follows:

$$\varepsilon = 1/R_0 - s_f \tag{4.1}$$

Since we focus on the limit $t_f \to \infty$, the system always ends up reaching herd immunity, with $s_f \leq 1/R_0$, so that $\varepsilon > 0$.

Non-behavioral limit: This case has a long history of being studied [1, 51–54]. In our framework, the known solution is obtained at $\alpha = 0$, where Equation (3.16) has the following solution:

$$s(r) = s_0 e^{-R_0(r-r_0)}. \tag{4.2}$$

At the final time, this evaluates to $s_f = e^{-R_0(1-s_f-r_0)}$. From this, we obtain the following:

$$s_f = -W(-s_0 R_0 e^{R_0(r_0-1)})/R_0, \tag{4.3}$$

where W is the principal branch of the Lambert W function, defined as the inverse of the function we^w [76]. This function is also called the product logarithm. Therefore, the excess cases are given by the following:

$$\varepsilon = (1 + W(-s_0 R_0 e^{R_0(r_0-1)}))/R_0. \tag{4.4}$$

The infection peak $\hat{i} = \max(i) = i(\hat{t})$ takes place at time $\hat{t}$ for which $di/dt = 0$. From Equation (2.3), we conclude that then also $s(\hat{t}) = 1/R_0$. We make use of this in order to solve Equation (4.2) for the infection peak and obtain the following:

$$\hat{i} = \max(i) = 1 - r_0 - (1 + \ln(s_0 R_0))/R_0 \tag{4.5}$$

These two results are independent of α and x. We see that they can describe the full analytic solution well for small α and x, see Figure 3.

Strong social distancing limit: This regime requires analysis of the limit $\alpha x \gg 1$. In this limit, ε ends up being small. Assuming that $s_0 > 1/R_0$, we obtain the asymptote for the excess cases by expanding Equation (3.18) in both $1/(\alpha x)$ and ε small and matching order by order to obtain the following:

$$\varepsilon = \frac{2}{x\alpha}. \tag{4.6}$$

For the infection peak, we analogously obtain

$$\hat{i} = \max(i) = \frac{2(R_0 - 1)}{xR_0\alpha}. \tag{4.7}$$

At large infection costs α, the solution does indeed approach both these asymptotes, see Figure 3.

Earlier, we claimed that it was not an issue that the social distancing cost remained finite at vanishing activity, $k \to 0$, since the solution would be unable to reach such values in any case. We can easily see that in the limit of large infection cost, $\alpha x \gg 1$, by combining Equations (3.15), (4.6), and (4.7), we can obtain the following:

$$R_b = R_0 - \frac{\alpha s_f}{2} xi \geq R_0 - \left(1 - 2\frac{R_0}{\alpha x}\right)(R_0 - 1) \geq 1. \tag{4.8}$$

This means that the shape of the social distancing cost function for $k < 1/R_0$ is irrelevant in this work.

Crossover costs allow for categorization of the expected behavioral response: Having obtained analytic expressions for the two extreme limits of behavior, we can calculate the approximate cost at which the transition between them occurs. This allows us to identify the infection cost at which a given disease would be expected to elicit a significant self-organized behavioral response from a population. It turns out that the the excess cases and the infection peak transition at different costs, $\alpha^\star_{ex}$ and $\alpha^\star_{peak}$, respectively. For the excess cases, the results for the non-behavioral and the strong social distancing limits, Equations (4.4) and (4.6), respectively, match at

$$\alpha^\star_{ex} = \frac{2}{x} \frac{R_0}{1 + (W(-s_0 R_0 e^{R_0(r_0-1)})}. \tag{4.9}$$

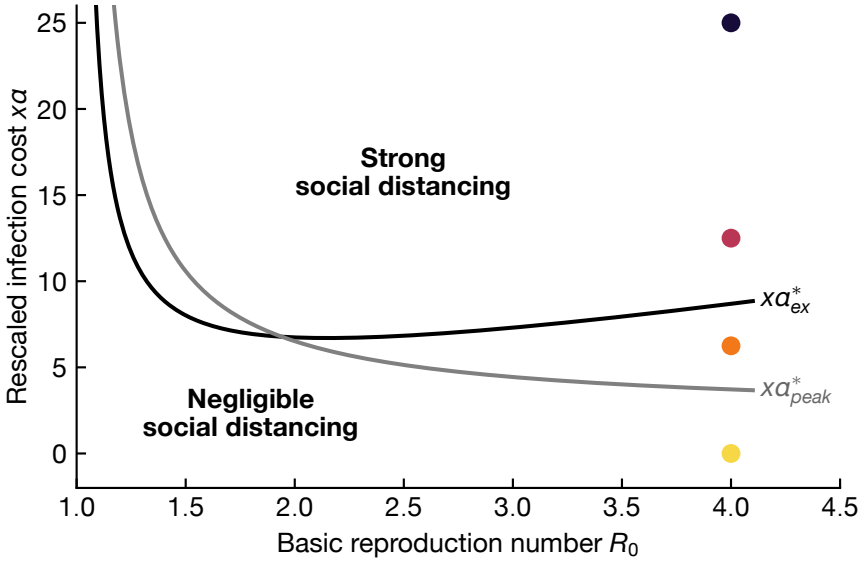

Figure 4. Crossover costs allow for categorization of the expected behavioral response. Characterization of the expected behavioral response in the space spanned by infection cost rescaled with effectiveness, $x\alpha$, and the basic reproduction number, R_0. The black line describes the critical cost $\alpha^\star_{ex}$ for the transition in the excess cases, see Equation (4.9). The grey line describes the critical cost $\alpha^\star_{peak}$ for the transition in the infection peak, see Equation (4.10). The dependence on x can be absorbed into a rescaling of these costs. For low $x\alpha$, the behavior is well represented by the non-behavioral limit. For large $x\alpha$ and large enough R_0, a strong behavioral modification is rational. The colored dots represent the parameter values used in Figure 1.

For the infection peak, we match Equations (4.5) and (4.7) and obtain the following:

$$\alpha^\star_{peak} = \frac{2}{x}\frac{R_0 - 1}{R_0(1 - r_0) - 1 - \ln(s_0 R_0)}. \tag{4.10}$$

These crossover costs identify the transition between the two regimes well, see Figure 3. In addition, along with the non-behavioral limits for the excess cases ε and the infection peak $\max(i)$, they can be used to collapse both quantities onto master curves very successfully, see Figure 3 insets. Together, both crossover costs determine different aspects of general population behavior and allow us to draw a "phase diagram" of social distancing, see Figure 4. If getting infected by a disease costs less than either of the two crossover costs, then the expected social distancing will be negligible. If the infection costs exceeds both costs, then one can expect a strong self-organized behavioral response. We note here the important role of the effectiveness x in scaling the crossover costs. If social distancing is perceived as being relatively ineffective, then the cost of the disease must be perceived much higher to elicit a strong behavioral response.

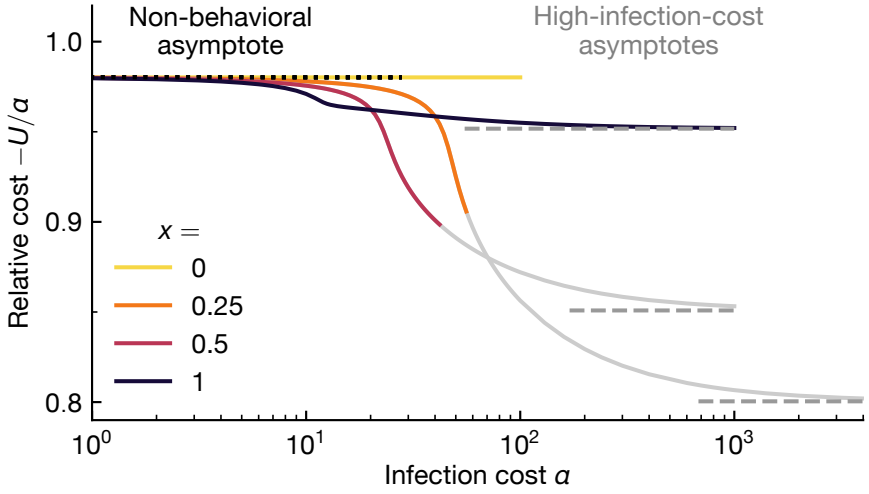

Figure 5. Total cost of the epidemic. The total epidemic cost with respect to the infection cost, $-U/\alpha$, as a function of infection cost α for a range of effectivenesses x. The corresponding non-behavioral, Equation (4.12), and strong social distancing asymptotes, Equation (4.13), are indicated by dotted and dashed lines, respectively. The light grey solid lines indicate where the solution does not represent a Nash equilibrium, as discussed in Section 4.1.

Behavioral modification reduces the total cost of the epidemic: We are also able to analytically calculate the utility, Equation (2.5), corresponding to a given equilibrium behavior

$$U = -\alpha\left[r_f - r_0 + \frac{xs_f}{2}\left(R_0(r_f - r_0) + \ln\left(\frac{s_f}{s_0}\right)\right)\right], \tag{4.11}$$

noting that s_f and $r_f = 1 - s_f$ depend on α, x, and R_0. This form exposes the two costs that contribute to the utility: the total cost due to infection is $-\alpha(r_f - r_0)$, while the cost due to social distancing makes up the rest. Additionally, the utility can be evaluated in the two previously discussed limits. Using Equation (4.3), the non-behavioral limit evaluates to

$$U = -\alpha\left[1 + \frac{1}{R_0}W\left(-s_0R_0e^{R_0(r_0-1)}\right) - r_0\right]. \tag{4.12}$$

In the strong social distancing limit, the utility asymptotically evaluates to, using $y = 1 - x$,

$$U = -\frac{x+2}{2}\alpha\left[1 - r_0 - \frac{1}{R_0} - \frac{x}{x+2}\frac{\ln(R_0s_0)}{R_0}\right]. \tag{4.13}$$

We find that the total cost of the epidemic is generally reduced by social distancing, see Figure 5. As we already saw earlier, the larger the effectiveness x of individual social distancing, the smaller are the crossover costs at which one expects strong social distancing. This is also apparent in the utility. Perhaps surprisingly, the possible reduction in the total epidemic cost tends to be more modest for larger x, even though the total number of cases is smaller, see Figure 3b. Clearly, this additional reduction in cases can only be achieved by relatively more expensive social distancing.

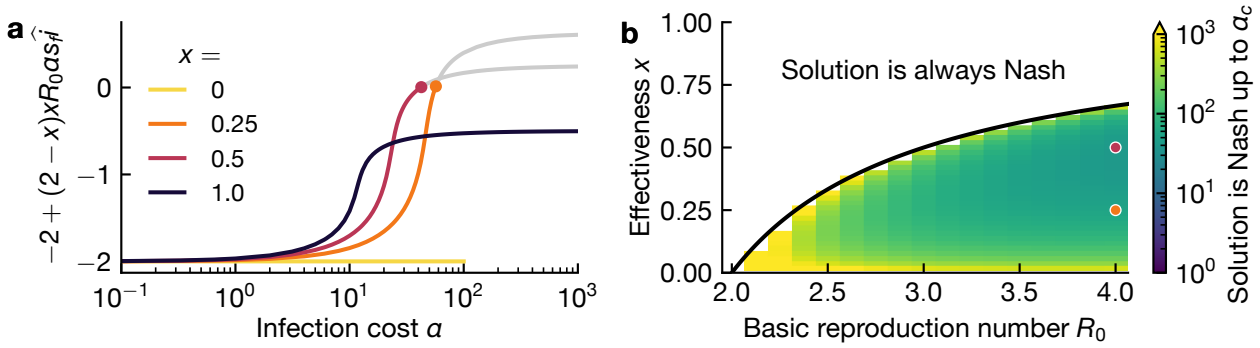

Figure 6. For some disease parameters, the solution is not a Nash equilibrium. (a) Plot of the maximum criterion, Equation (4.14), as a function of infection cost α and effectiveness x. The solution represents a Nash equilibrium as long as this expression is negative. For $R_0 = 4$, as shown here, the solution is only a Nash equilibrium for all α if $x \geq 2/3$, see Equation (4.16). For values below this threshold, there exists an α_c above which our solution ceases to be an equilibrium, see colored dots. The solution is greyed out where it does not represent a Nash equilibrium. (b) Plot of α_c, the infection cost α values for which the maximum criterion, Equation (4.14), evaluates to 0 and the solution is therefore still a Nash equilibrium for all $\alpha < \alpha_c$. Above the black line the solution is always Nash, Equation (4.16). For the two cases in panel (a) where the solution is not Nash, we have marked the parameter values with colored dots for convenience.

4.1. Establishing when the candidate solution is a Nash equilibrium

The variational approach used by us only yields conditions sufficient to identify extrema. In order for the solution to represent a Nash equilibrium, we require that it be a maximum. This holds if $\partial^2 H/\partial\kappa^2 < 0$. For $x + y = z = 1$, $x \in [0, 1]$, and using $k > 0$, we can show that

$$k \left.\frac{\partial^2 H}{\partial \kappa^2}\right|_{\kappa=k} = -2 + (2 - x)x\, R_0\, \alpha\, s_f\, i \tag{4.14}$$

Numerically, we confirm that this criterion increases with α for fixed R_0 and x, see Figure 6a. Therefore, the criterion is not always negative. Analytically, we can study the non-behavioral and strong social distancing limits. In the non-behavioral limit, $\alpha = 0$, and so we find trivially that $\partial^2 H/\partial\kappa^2 = -2 < 0$. In the high infection cost limit, using Equations (4.6) and (4.7), we find that

$$\begin{aligned} k \left.\frac{\partial^2 H}{\partial \kappa^2}\right|_{\kappa=k} &= -2 + (2 - x)xR_0\alpha s_f i \\ \leq -2 + (2 - x)xR_0\alpha s_f \hat{i} &\approx -2 + (2 - x)\left(\frac{1}{R_0} - \frac{2}{x\alpha}\right)2(R_0 - 1). \end{aligned} \tag{4.15}$$

Therefore, in the limit of $\alpha \to \infty$, in which the asymptotic expressions Equations (4.6) and (4.7) become exact, a necessary condition for our solution to be a Nash equilibrium is that

$$x \geq x_c = \frac{R_0 - 2}{R_0 - 1}. \tag{4.16}$$

This indicates that for $R_0 > 2$, our solution is not an equilibrium for all α and all $x \in [0, 1]$. However, for any given value of $x < x_c$, there is a range of α with an upper bound α_c for which the solution still represents a Nash equilibrium, see Figure 6. We cannot rule out the existence of another Nash equilibrium, possibly on the boundary of the control space. It is possible that above the threshold α_c, the analytical solution is replaced by a corner solution. One possible candidate would be the constant solution $k = 1/R_0$. However, we have not obtained evidence that this candidate represents a Nash equilibrium. This is probably a very subtle question in the limit of infinite t_f.

5. Discussion and conclusion

We extended an SIR compartmentalized model for disease dynamics discussed in an earlier work [56] to contain a more realistic expression for infection dynamics. In particular, we accounted for the fact that, in general, both susceptible and infectious social distancing behaviors would affect the likelihood of infection of the susceptible. Reassuringly, we were able to generalize the analytic solution identified in that earlier work to the more realistic modeling of infection dynamics presented here.

The new results are best understood in terms of a central parameter, the effectiveness x of susceptible social distancing. For $x = 1$, in which the infectious cannot affect the probability of infecting others, the previous results [56] are recovered. For $x = 0$, no behavioral modification is observed, since susceptible individuals cannot affect the probability of getting infected. In that case, the model reduces to well-known results without time-varying behavior [1, 51–54]. Most real diseases will correspond to scenarios in-between these extreme cases, in which both the infectious and the susceptible behaviors affect the likelihood of the susceptible becoming infected.

The higher the effectiveness x, the higher the cost of the disease α, and the higher the current number of cases, the stronger the social distancing can be expected. We are able to capture this in a simple rule, Equation (3.15). This result can be seen as justification for other models in which similar behavioral dynamics were assumed ad-hoc [2, 7, 8, 77]. For instance, behavior adjusting to infection levels were used to understand the HIV epidemic [78, 79]. For HIV, our assumption of initially asymptomatic infections that carry a high long-term cost is especially well suited.

We further exploit the analytic solution to generalize asymptotic expressions for the final number of cases in excess of herd immunity, Equation (4.6), the peak of infection, Equation (4.7), and the total cost of the epidemic, Equation (4.13), in the limit of high effectiveness of social distancing and a high infection cost. Additionally, we generalize the characteristic infection costs above which one expects to observe strong self-organized social distancing to include the effectiveness x of social distancing and find that the costs scale inversely proportionally to x.

We discover that our solution does not represent a Nash equilibrium for all parameter choices. The equilibrium is retained if either the effectiveness is large or the infection cost and basic reproduction are not too large. This may be a generic feature in models that feature a nonlinear dependence on the behavior in the disease dynamics or have non-quadratic social distancing costs.

While the presented model contains a sophisticated modeling of the infection dynamics, it is still highly idealized. Therefore, it is unlikely that it would yield quantitative predictions in the case of an actual epidemic. Still, the results here may serve as helpful approximations to guide individual and policy responses. The benefit of using such a simple model with an analytic solution is that it allows us to break down a complex optimization problem into a few key results. First, we were able to derive

a heuristic for how equilibrium social distancing loosely depends on the current status of an epidemic and its disease properties. This would likely hold approximately in real epidemics and similar rules have been used in other models, albeit without the game-theoretic support provided here. Second, we identified the characteristic costs that allow one to estimate whether a population will meaningfully engage in spontaneous social distancing without for government intervention. We believe that it is helpful to provide this intuition to individuals and government decision makers alike.

Use of AI tools declaration

The authors declare they have not used Artificial Intelligence (AI) tools in the creation of this article.

Acknowledgments

This work was supported by Grants-in-Aid for Scientific Research (JSPS KAKENHI) under Grants No. 22K14012 (SKS), 25H01365 (SKS, TJK), 25H01536 (JJM), 25K03185 (JJM), 25H01476 (RY), and the JSPS Core-to-Core Program "Advanced core-to-core network for the physics of self-organizing active matter" JPJSCCA20230002 (SKS, JJM, RY, MST). MST acknowledges the generous support of Royal Society/JSPS International Exchanges Cost Share award IEC\R3\223006 and the kind hospitality of the Yamamoto group. Part of this research was conducted while visiting the Okinawa Institute of Science and Technology (OIST) through the Theoretical Sciences Visiting Program (TSVP) Thematic Program on Biological Information Processing (TP24BI). The funders had no role in study design, data collection and analysis, decision to publish, or preparation of the manuscript.

Conflict of interest

The authors declare there is no conflict of interest.

References

1. W. O. Kermack, A. McKendrick, A contribution to the mathematical theory of epidemics, *Proc. R. Soc. A*, **115** (1927), 700–721. https://doi.org/10.1098/rspa.1927.0118
2. V. Capasso, G. Serio, A generalization of the Kermack-McKendrick deterministic epidemic model, *Math. Biosci.*, **42** (1978), 43–61. https://doi.org/10.1016/0025-5564(78)90006-8
3. T. C. Reluga, Game Theory of Social Distancing in Response to an Epidemic, *PLoS Comput. Biol.*, **6** (2010), e1000793. https://doi.org/10.1371/journal.pcbi.1000793
4. E. P. Fenichel, C. Castillo-Chavez, M. G. Ceddia, G. Chowell, P. A. G. Parra, G. J. Hickling, et al., Adaptive human behavior in epidemiological models, *Proc. Natl. Acad. Sci.*, **108** (2011), 6306–6311. https://doi.org/10.1073/pnas.1011250108
5. Y. Yan, A. A. Malik, J. Bayham, E. P. Fenichel, C. Couzens, S. B. Omer, Measuring voluntary and policy-induced social distancing behavior during the COVID-19 pandemic, *Proc. Natl. Acad. Sci.*, **118** (2021), e2008814118. https://doi.org/10.1073/pnas.2008814118
6. P. Dönges, J. Wagner, S. Contreras, E. N. Iftekhar, S. Bauer, S. B. Mohr, et al., Interplay

Between Risk Perception, Behavior, and COVID-19 Spread, *Front. Phys.*, **10** (2022), 1–12. https://doi.org/10.3389/fphy.2022.842180

7. S. Funk, M. Salathé, V. A. Jansen, Modelling the influence of human behaviour on the spread of infectious diseases: A review, *J. R. Soc. Interface*, **7** (2010), 1247–1256. https://doi.org/10.1098/rsif.2010.0142
8. Piero Manfredi, Alberto D'Onofrio, *Modeling the Interplay Between Human Behavior and the Spread of Infectious Diseases*, Springer New York, New York, NY (2013). https://doi.org/10.1007/978-1-4614-5474-8
9. Z. Wang, C. T. Bauch, S. Bhattacharyya, A. D'Onofrio, P. Manfredi, M. Perc, et al., Statistical physics of vaccination, *Phys. Rep.*, **664** (2016), 1–113. https://doi.org/10.1016/j.physrep.2016.10.006
10. F. Verelst, L. Willem, P. Beutels, Behavioural change models for infectious disease transmission: A systematic review (2010–2015), *J. R. Soc. Interface*, **13** (2016). https://doi.org/10.1098/rsif.2016.0820
11. S. L. Chang, M. Piraveenan, P. Pattison, M. Prokopenko, Game theoretic modelling of infectious disease dynamics and intervention methods: A review, *J. Biol. Dyn.*, **14** (2020), 57–89. https://doi.org/10.1080/17513758.2020.1720322
12. A. Reitenbach, F. Sartori, S. Banisch, A. Golovin, A. Calero Valdez, M. Kretzschmar, et al., Coupled infectious disease and behavior dynamics. A review of model assumptions, *Rep. Prog. Phys.*, **88** (2024). https://doi.org/10.1088/1361-6633/ad90ef
13. N. Gozzi, N. Perra, A. Vespignani, Comparative evaluation of behavioral epidemic models using COVID-19 data, *Proc. Natl. Acad. Sci.*, **122** (2025), e2421993122. https://doi.org/10.1073/pnas.2421993122
14. L. Müller, P. Mallick, A. B. Marín-Carballo, P. Dönges, R. J. N. Kettlitz, C. J. Klett-Tammen, et al., Testing paradox may explain increased observed prevalence of bacterial stis among msm on hiv prep: A modeling study, *Proc. Natl. Acad. Sci.*, **122** (2025), 2524944122. https://doi.org/10.1073/pnas.2524944122
15. E. M. Hill, M. Ryan, D. Haw, M. P. Lynch, R. McCabe, A. E. Milne, et al., Integrating human behaviour and epidemiological modelling: unlocking the remaining challenges, *Math. Med. Life Sci.*, **1** (2024). https://doi.org/10.1080/29937574.2024.2429479
16. T. Philipson, Chapter 33 Economic epidemiology and infectious diseases, in: *Handbook of Health Economics* (eds. A. Culyer, J. Newhouse). Elsevier Science B. V. (2000), 1761–1799. https://doi.org/10.1016/S1574-0064(00)80046-3
17. T. C. Reluga, J. Li, Games of age-dependent prevention of chronic infections by social distancing, *J. Math. Biol.*, **66** (2013), 1527–1553. https://doi.org/10.1007/s00285-012-0543-8
18. D. Acemoglu, V. Chernozhukov, I. Werning, M. D. Whinston, Optimal Targeted Lockdowns in a Multigroup SIR Model, *Am. Econ. Rev. Insights*, **3** (2021), 487–502. https://doi.org/10.1257/aeri.20200590
19. M. Makris, Covid and social distancing with a heterogenous population, *Econ. Theory*, **77** (2024), 445–494. https://doi.org/10.1007/s00199-021-01377-2
20. M. J. Tildesley, A. Vassall, S. Riley, M. Jit, F. Sandmann, E. M. Hill, et al., Optimal

health and economic impact of non-pharmaceutical intervention measures prior and post vaccination in England: a mathematical modelling study, *R. Soc. Open Sci.*, **9** (2022), 211746. https://doi.org/10.1098/rsos.211746

21. M. J. Keeling, L. Dyson, M. J. Tildesley, E. M. Hill, S. Moore, Comparison of the 2021 COVID-19 roadmap projections against public health data in England, *Nat. Commun.*, **13** (2022), 4924. https://doi.org/10.1038/s41467-022-31991-0
22. C. I. Huang, R. E. Crump, P. E. Brown, S. E. Spencer, E. M. Miaka, C. Shampa et al., Identifying regions for enhanced control of gambiense sleeping sickness in the Democratic Republic of Congo, *Nat. Commun.*, **13** (2022), 1–11. https://doi.org/10.1038/s41467-022-29192-w
23. N. M. Ferguson, D. A. T. Cummings, C. Fraser, J. C. Cajka, P. C. Cooley, D. S. Burke, Strategies for mitigating an influenza pandemic, *Nature*, **442** (2006), 448–452. https://doi.org/10.1038/nature04795
24. J. Tanimoto, Social Dilemma Analysis of the Spread of Infectious Disease, in: *Evol. Games with Sociophysics*. Springer, Singapore, (2018), 155–216. https://doi.org/10.1007/978-981-13-2769-8_4
25. P. Mellacher, COVID-Town: An Integrated Economic-Epidemiological Agent-Based Model, GSC discussion papers, (2020). Available from: `https://ideas.repec.org/p/pra/mprapa/103661.html`
26. J. Grauer, H. Löwen, B. Liebchen, Strategic spatiotemporal vaccine distribution increases the survival rate in an infectious disease like Covid-19, *Sci. Rep.*, **10** (2020), 1–10. https://doi.org/10.1038/s41598-020-78447-3
27. P. Holme, J. Saramäki, Temporal networks, *Phys. Rep.*, **519** (2012), 97–125. https://doi.org/10.1016/j.physrep.2012.03.001
28. P. Holme, N. Masuda, The basic reproduction number as a predictor for epidemic outbreaks in temporal networks, *PLoS One*, **10** (2015), 1–15. https://doi.org/10.1371/journal.pone.0120567
29. A. G. Chandrasekhar, P. Goldsmith-Pinkham, M. O. Jackson, S. Thau, Interacting regional policies in containing a disease, *Proc. Natl. Acad. Sci.*, **118** (2021), e2021520118. https://doi.org/10.1073/pnas.2021520118
30. D. He, J. Dushoff, T. Day, J. Ma, D. J. Earn, Inferring the causes of the three waves of the 1918 influenza pandemic in England and Wales, *Proc. R. Soc. B Biol. Sci.*, **280** (2013), 20131345. https://doi.org/10.1098/rspb.2013.1345
31. K. Prem, A. R. Cook, M. Jit, Projecting social contact matrices in 152 countries using contact surveys and demographic data, *PLOS Comput. Biol.*, **13** (2017), e1005697. https://doi.org/10.1371/journal.pcbi.1005697
32. J. Mossong, N. Hens, M. Jit, P. Beutels, K. Auranen, R. Mikolajczyk et al., Social contacts and mixing patterns relevant to the spread of infectious diseases, *PLoS Med.*, **5** (2008), 0381–0391. https://doi.org/10.1371/journal.pmed.0050074
33. M. J. Tildesley, T. A. House, M. C. Bruhn, R. J. Curry, M. O'Neil, J. L. Allpress et al., Impact of spatial clustering on disease transmission and optimal control, *Proc. Natl. Acad. Sci.*, **107** (2010), 1041–1046. https://doi.org/10.1073/pnas.0909047107
34. K. Sun, W. Wang, L. Gao, Y. Wang, K. Luo, L. Ren, et al., Transmission hetero-

geneities, kinetics, and controllability of SARS-CoV-2, *Science*, **371** (2021), eabe2424. https://doi.org/10.1126/science.abe2424

35. E. M. Hill, N. S. Prosser, P. E. Brown, E. Ferguson, M. J. Green, J. Kaler, et al., Incorporating heterogeneity in farmer disease control behaviour into a livestock disease transmission model, *Prev. Vet. Med.*, **219** (2023), 106019. https://doi.org/10.1016/j.prevetmed.2023.106019
36. P. Dönges, T. Götz, N. Kruchinina, T. Krüger, K. Niedzielewski, V. Priesemann, et al., Sir Model for Households, *SIAM J. Appl. Math.*, **84** (2024), 1460–1481. https://doi.org/10.1137/23M1556861
37. C. Giannitsarou, S. Kissler, F. Toxvaerd, Waning Immunity and the Second Wave: Some Projections for SARS-CoV-2, *Am. Econ. Rev. Insights*, **3** (2021), 321–338. https://doi.org/10.1257/aeri.20200343
38. F. J. Schwarzendahl, J. Grauer, B. Liebchen, H. Löwen, Mutation induced infection waves in diseases like COVID-19, *Sci. Rep.*, **12** (2022), 1–11. https://doi.org/10.1038/s41598-022-13137-w
39. J. Yong, X. Y. Zhou, *Stochastic controls: Hamiltonian systems and HJB equations*, Springer Science & Business Media, (1999). https://doi.org/10.1007/978-1-4612-1466-3
40. T. Tottori, T. J. Kobayashi, Memory-limited partially observable stochastic control and its mean-field control approach, *Entropy*, **24** (2022), 1–27. https://doi.org/10.3390/e24111599
41. T. Tottori, T. J. Kobayashi, Theory for optimal estimation and control under resource limitations and its applications to biological information processing and decision-making, *Phys. Rev. Res.*, **7** (2025), 043048. https://doi.org/10.1103/gvl6-cvby
42. S. A. Horiguchi, T. J. Kobayashi, Optimal control of stochastic reaction networks with entropic control cost and emergence of mode-switching strategies, *PRX Life*, **3** (2025), 033027. https://doi.org/10.1103/zttn-tpzq
43. M. Barnett, G. Buchak, C. Yannelis, Epidemic responses under uncertainty, *Proc. Natl. Acad. Sci.*, **120** (2023), e2208111120. https://doi.org/10.1073/pnas.2208111120
44. K. Shea, R. K. Borchering, W. J. M. Probert, E. Howerton, T. L. Bogich, S.-L. Li, et al., Multiple models for outbreak decision support in the face of uncertainty, *Proc. Natl. Acad. Sci.*, **120** (2023), e2207537120. https://doi.org/10.1073/pnas.2207537120
45. F. Toxvaerd, R. Rowthorn, On the management of population immunity, *J. Econ. Theory*, **204** (2022), 105501. https://doi.org/10.1016/j.jet.2022.105501
46. S. Moore, E. M. Hill, L. Dyson, M. J. Tildesley, M. J. Keeling, Modelling optimal vaccination strategy for SARS-CoV-2 in the UK, *PLoS Comput. Biol.*, **17** (2021), 1–20. https://doi.org/10.1371/journal.pcbi.1008849
47. A. J. Kucharski, P. Klepac, A. J. Conlan, S. M. Kissler, M. L. Tang, H. Fry, et al., Effectiveness of isolation, testing, contact tracing, and physical distancing on reducing transmission of SARS-CoV-2 in different settings: A mathematical modelling study, *Lancet Infect. Dis.*, **20** (2020), 1151–1160. https://doi.org/10.1016/S1473-3099(20)30457-6
48. S. Contreras, J. Dehning, M. Loidolt, J. Zierenberg, F. P. Spitzner, J. H. Urrea-Quintero, et al., The challenges of containing SARS-CoV-2 via test-trace-and-isolate, *Nat. Commun.*, **12** (2021), 1–13. https://doi.org/10.1038/s41467-020-20699-8

49. S. Contreras, J. Dehning, S. B. Mohr, S. Bauer, F. Paul Spitzner, V. Priesemann, Low case numbers enable long-term stable pandemic control without lockdowns, *Sci. Adv.*, **7** (2021), eabg2243. https://doi.org/10.1126/sciadv.abg2243
50. D. Roberts, E. Jamrozik, G. S. Heriot, A. C. Slim, M. J. Selgelid, J. C. Miller, Quantifying the impact of individual and collective compliance with infection control measures for ethical public health policy, *Sci. Adv.*, **9** (2023), eabn7153. https://doi.org/10.1126/sciadv.abn7153
51. J. C. Miller, A Note on the Derivation of Epidemic Final Sizes, *Bull. Math. Biol.*, **74** (2012), 2125–2141. https://doi.org/10.1007/s11538-012-9749-6
52. T. Harko, F. S. Lobo, M. K. Mak, Exact analytical solutions of the Susceptible-Infected-Recovered (SIR) epidemic model and of the SIR model with equal death and birth rates, *Appl. Math. Comput.*, **236** (2014), 184–194. https://doi.org/10.1016/j.amc.2014.03.030
53. J. C. Miller, Mathematical models of SIR disease spread with combined non-sexual and sexual transmission routes, *Infect. Dis. Model.*, **2** (2017), 35–55. https://doi.org/10.1016/j.idm.2016.12.003
54. M. Kröger, R. Schlickeiser, Analytical solution of the SIR-model for the temporal evolution of epidemics. Part A: Time-independent reproduction factor, *J. Phys. A Math. Theor.*, **53** (2020), 505601. https://doi.org/10.1088/1751-8121/abc65d
55. I. S. Pacheco, C. A. M. C. Junior, D. A. Stariolo, Semianalytical solution of seir-like models of epidemic spreading, *Phys. Rev. E*, **111** (2025), 064305. https://doi.org/10.1103/fwx4-m2wg
56. S. K. Schnyder, J. J. Molina, R. Yamamoto, M. S. Turner, Understanding Nash epidemics, *Proc. Natl. Acad. Sci.*, **122** (2025), e2409362122. https://doi.org/10.1073/pnas.2409362122
57. M. Makris, F. Toxvaerd, Great Expectations: Social Distancing in Anticipation of Pharmaceutical Innovations, Cambridge Work. Pap. Econ., (2020). https://doi.org/10.17863/CAM.62310
58. R. Rowthorn, F. Toxvaerd, The optimal control of infectious diseases via prevention and treatment, Cambridge Work. Pap. Econ., (2020). https://doi.org/10.17863/CAM.52481
59. S. L. Li, O. N. Bjørnstad, M. J. Ferrari, R. Mummah, M. C. Runge, C. J. Fonnesbeck, et al., Essential information: Uncertainty and optimal control of Ebola outbreaks, *Proc. Natl. Acad. Sci.*, **114** (2017), 5659–5664. https://doi.org/10.1073/pnas.1617482114
60. Z. A. Bethune, A. Korinek, COVID-19 infection externalities: Trading off lives vs. livelihoods, NBER working paper series, (2020). Available from: http://www.nber.org/papers/w27009
61. A. Aurell, R. Carmona, G. Dayanikli, M. Laurière, Optimal Incentives to Mitigate Epidemics: A Stackelberg Mean Field Game Approach, *SIAM J. Control Optim.*, **60** (2022), S294–S322. https://doi.org/10.1137/20M1377862
62. S. K. Schnyder, J. J. Molina, R. Yamamoto, M. S. Turner, Rational social distancing policy during epidemics with limited healthcare capacity, *PLoS Comput. Biol.*, **19** (2023), e1011533. https://doi.org/10.1371/journal.pcbi.1011533
63. B. M. Althouse, T. C. Bergstrom, C. T. Bergstrom, A public choice framework for controlling transmissible and evolving diseases, *Proc. Natl. Acad. Sci.*, **107** (2010), 1696–1701. https://doi.org/10.1073/pnas.0906078107
64. A. Bensoussan, J. Frehse, P. Yam, *Mean Field Games and Mean Field Type Control Theory*, Springer, (2013). https://doi.org/10.1007/978-1-4614-8508-7

65. R. Carmona, F. Delarue, *Probabilistic Theory of Mean Field Games with Applications I*, Springer, (2018). https://doi.org/10.1007/978-3-319-58920-6
66. M. S. Eichenbaum, S. Rebelo, M. Trabandt, The Macroeconomics of Epidemics, *Rev. Financ. Stud.*, **34** (2021), 5149–5187. https://doi.org/10.1093/rfs/hhab040
67. D. McAdams, Nash SIR: An Economic-Epidemiological Model of Strategic Behavior During a Viral Epidemic, *SSRN Electron. J.* (2020). https://doi.org/10.2139/ssrn.3593272
68. F. Toxvaerd, Equilibrium Social Distancing, *Cambridge Work. Pap. Econ.*, **8** (2020). Available from: `https://www.econ.cam.ac.uk/publications/cwpe/2021`
69. S. K. Schnyder, J. J. Molina, R. Yamamoto, M. S. Turner, Rational social distancing in epidemics with uncertain vaccination timing, *PLoS One*, **18** (2023), e0288963. https://doi.org/10.1371/journal.pone.0288963
70. A. D'Onofrio, P. Manfredi, P. Poletti, The Interplay of Public Intervention and Private Choices in Determining the Outcome of Vaccination Programmes, *PLoS One*, **7** (2012), e45653. https://doi.org/10.1371/journal.pone.0045653
71. C. Chen, G. Kaur, A. Adiga, B. Espinoza, S. Venkatramanan, A. Warren, et al., Wastewater-based Epidemiology for COVID-19 Surveillance: A Survey, *Epidemics*, **49** (2024), 100793. https://doi.org/10.1016/j.epidem.2024.100793
72. T. C. Reluga, A. P. Galvani, A general approach for population games with application to vaccination, *Math. Biosci.*, **230** (2011), 67–78. https://doi.org/10.1016/j.mbs.2011.01.003
73. S. Lenhart, J. Workman, *Optimal Control Applied to Biological Models*, Chapman and Hall/CRC, (2007). https://doi.org/10.1201/9781420011418
74. L. S. Pontryagin, *The Mathematical Theory of Optimal Processes*, Routledge, (1987). https://doi.org/10.1201/9780203749319
75. M. Cadoni, How to reduce epidemic peaks keeping under control the time-span of the epidemic, *Chaos Soliton Fract.*, **138** (2020), 109940. https://doi.org/10.1016/j.chaos.2020.109940
76. R. M. Corless, G. H. Gonnet, D. E. G. Hare, D. J. Jeffrey, D. E. Knuth, On the Lambert W Function, *Adv. Comput. Math.*, **5** (1996), 329–359. https://doi.org/10.1007/BF02124750
77. J. Wagner, S. Bauer, S. Contreras, L. Fleddermann, U. Parlitz, V. Priesemann, Societal self-regulation induces complex infection dynamics and chaos, *Phys. Rev. Res.*, **7** (2025), 013308. https://doi.org/10.1103/PhysRevResearch.7.013308
78. K. P. Hadeler, C. Castillo-Chavez, A core group model for disease transmission, *Math. Biosci.*, **128** (1995), 41–55. https://doi.org/10.1016/0025-5564(94)00066-9
79. M. Kremer, Integrating behavioral choice into epidemiological models of aids, *Q. J. Econ.*, **111** (1996), 549–573. https://doi.org/10.2307/2946687

Appendix

In the main text, we discussed how to make progress in analysing the optimality condition on κ, Equation (2.15). While we required $z = x + y$, there are other possible choices for which one can make limited analytic progress. However, as far as we are aware, no complete analytic solutions are then possible. These other choices for the exponents lead to a social distancing cost that is no longer

quadratic in $R_b - R_0$, as in Equation (2.18). Provided $z \neq 1$ and $k > 0$, one can show that Equation (2.15) corresponds to

$$0 = k^z - 1 + (v_s - v_i)R_0 \frac{x}{2z} k^{x+y-z} si \tag{5.1}$$

By inspection there are certain combinations of x, y, z that lead to polynomials expressions that have explicit solutions for k. For example, assuming $2z = x + y$ yields

$$R_b = R_0 k^{x+y} = \frac{R_0}{(1 + \frac{x}{x+y} R_0 \alpha s_f i)^2} \tag{5.2}$$

Such analytic results serve as relatively simple heuristics for R_b. However, they do not allow for full analytic solutions for the disease dynamics.

AIMS Press